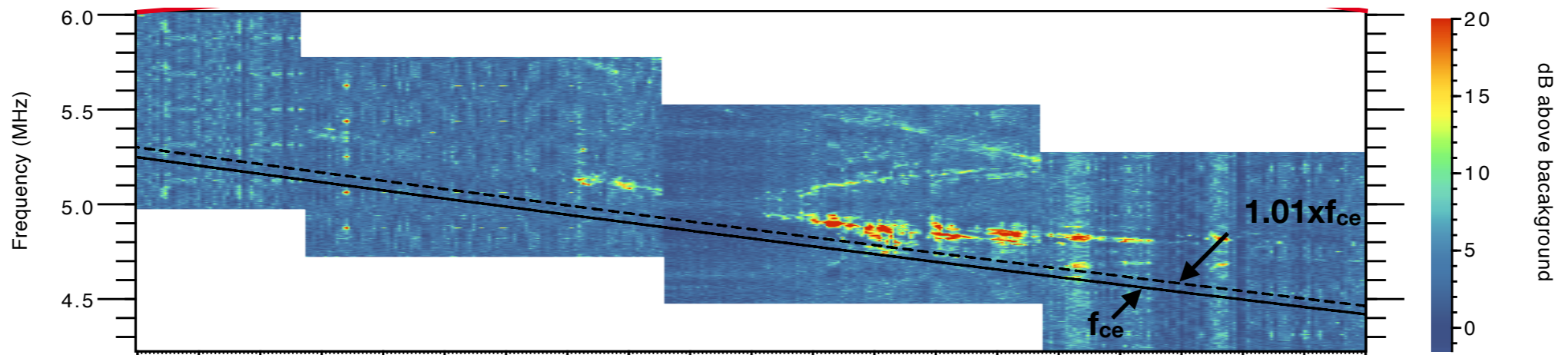


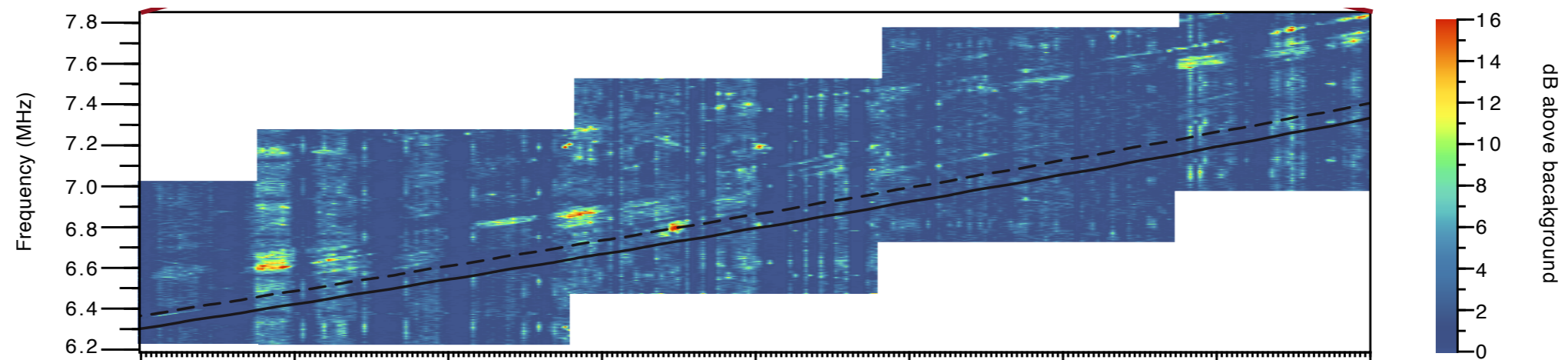
Moon-induced auroral radio emission in the Jovian system: in-situ measurements

C. K. Louis, P. Louarn, F. Allegrini, W. S. Kurth, J. Szalay

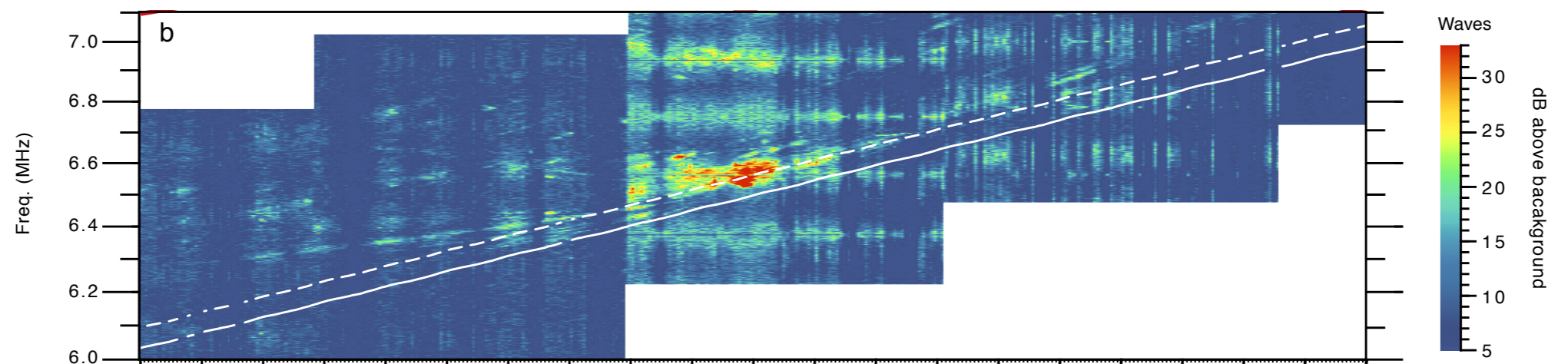
Io



Europa



Ganymede



Juno/Waves

Context

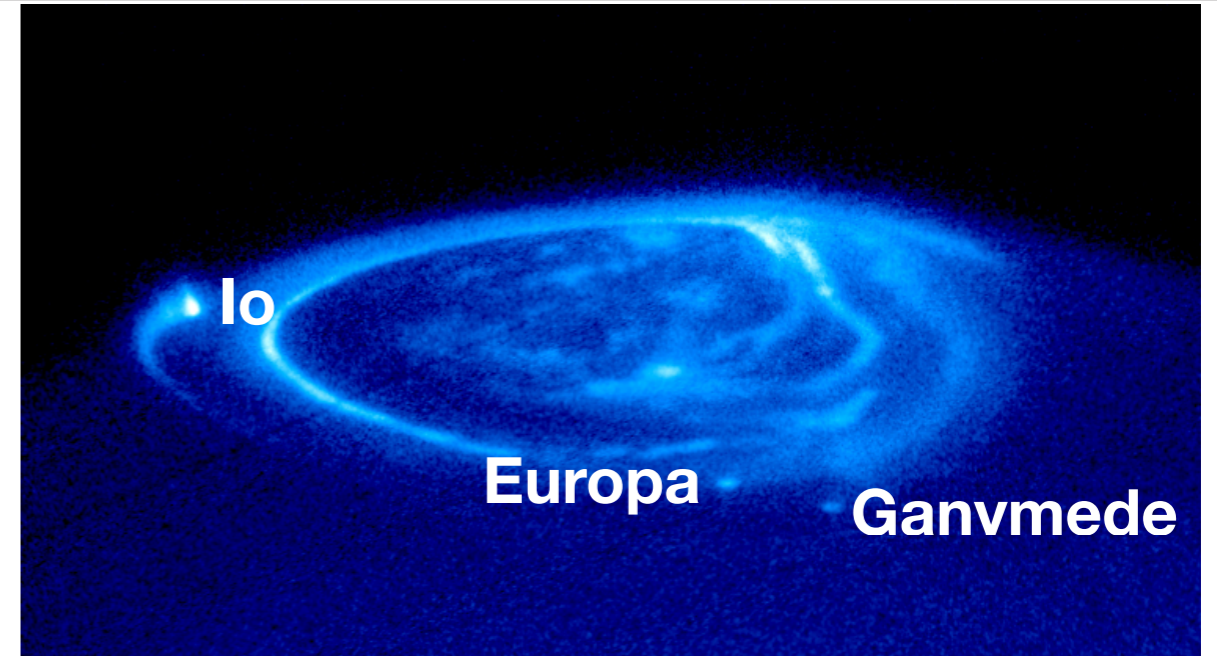
The Galilean moon-induced FUV emission:

Io [Prangé et al., 1996, Clarke et al., 1998]

Europa [Clarke et al., 2002]

Ganymede [Clarke et al., 2002]

Callisto [Bhattacharyya et al., 2018]



The Galilean moon-induced radio emission:

Io [Bigg 1954]

Europa [Louis et al., 2017]

Ganymede [Louis et al., 2017, Zarka et al., 2017, 2018]

Callisto (?) [Menietti et al., 2001, Higgins, 2007]



Emission produced at:

$$\omega = 2\pi f = \omega_{ce} \Gamma_r^{-1} + k_{||} v_{r||}$$

i.e. $\sim f_{ce}$ (up to few % $> f_{ce}$)

Radio emission characteristics ?

Resonant electrons energy ?

Aperture of the beaming angle ?

Link between radio and UV emissions?

Io: produced by Alfvénic interaction, radio emission above MAW and RAW FUV spot [Hess et al., 2010]

Europa & Ganymede: FUV emissions observed at the moon's footprint and along the moon's tail footprint [Bonfond et al., 2017a,b], but no simultaneous observation of FUV and radio emissions

Ganymede's tail flux tube crossing

- Ganymede's tail flux tube crossing: 07:37:14 - 07:37:32 [Szalay et al., 2020a]
- FUV emission observed, sustained by Alfvénic acceleration processes

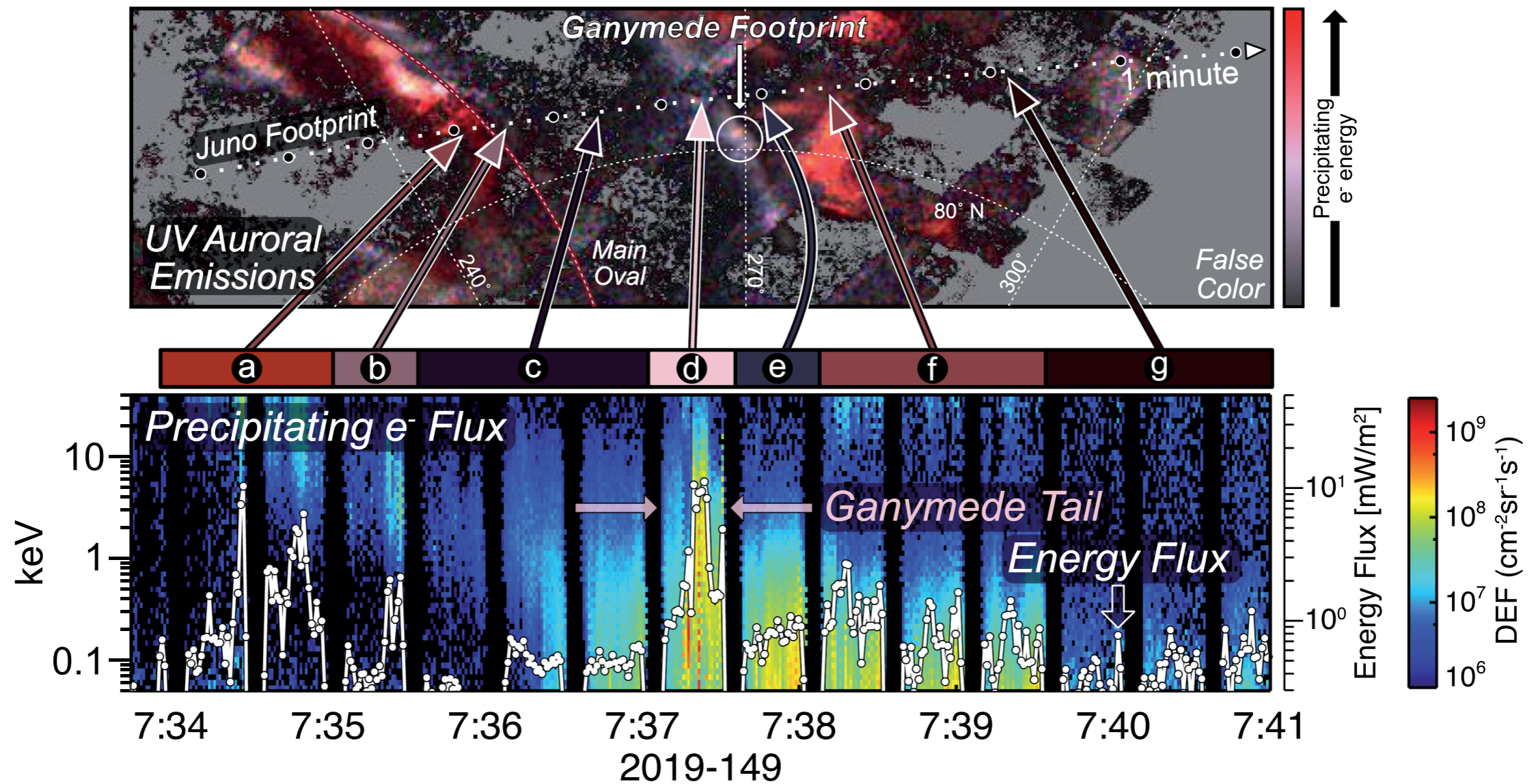
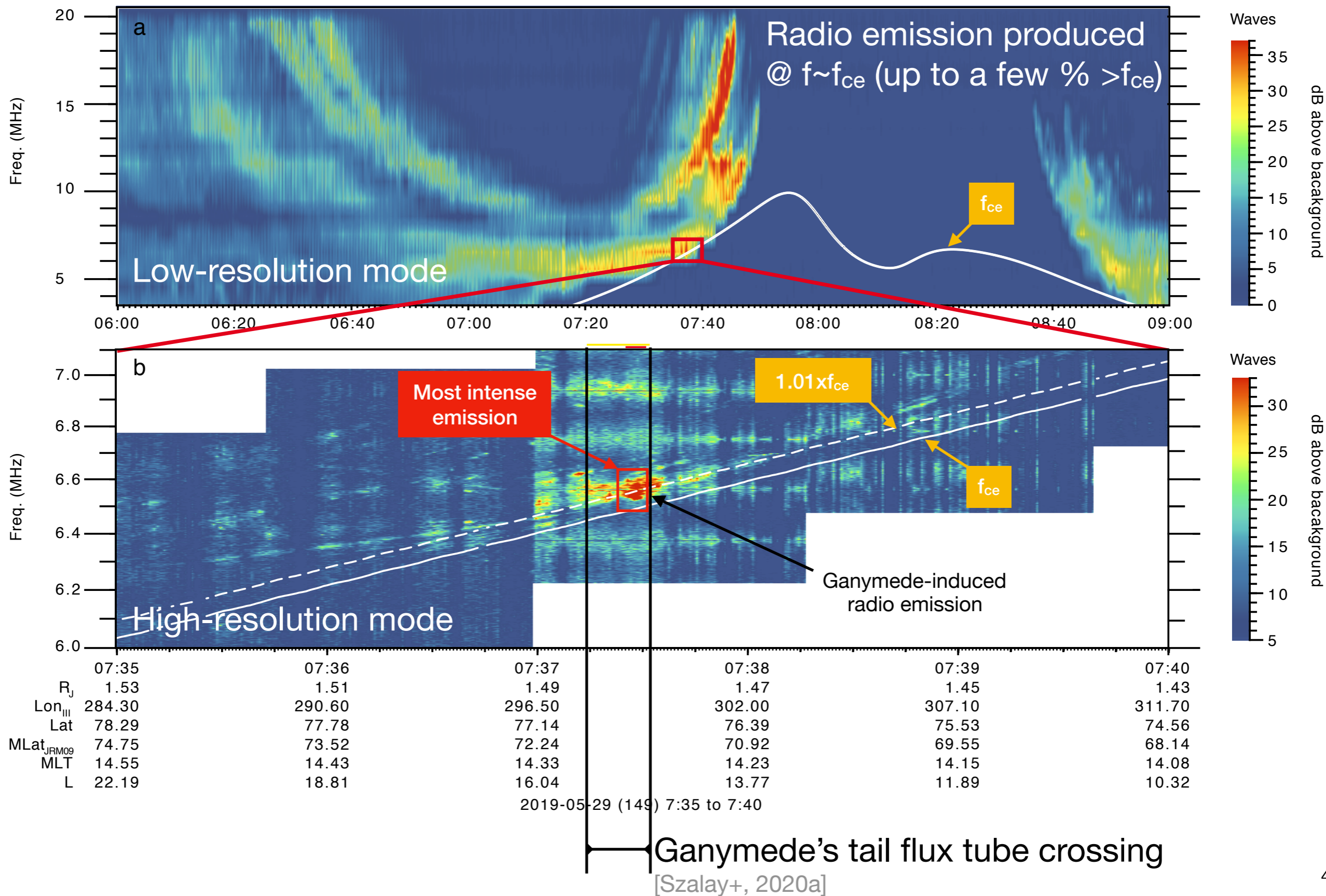


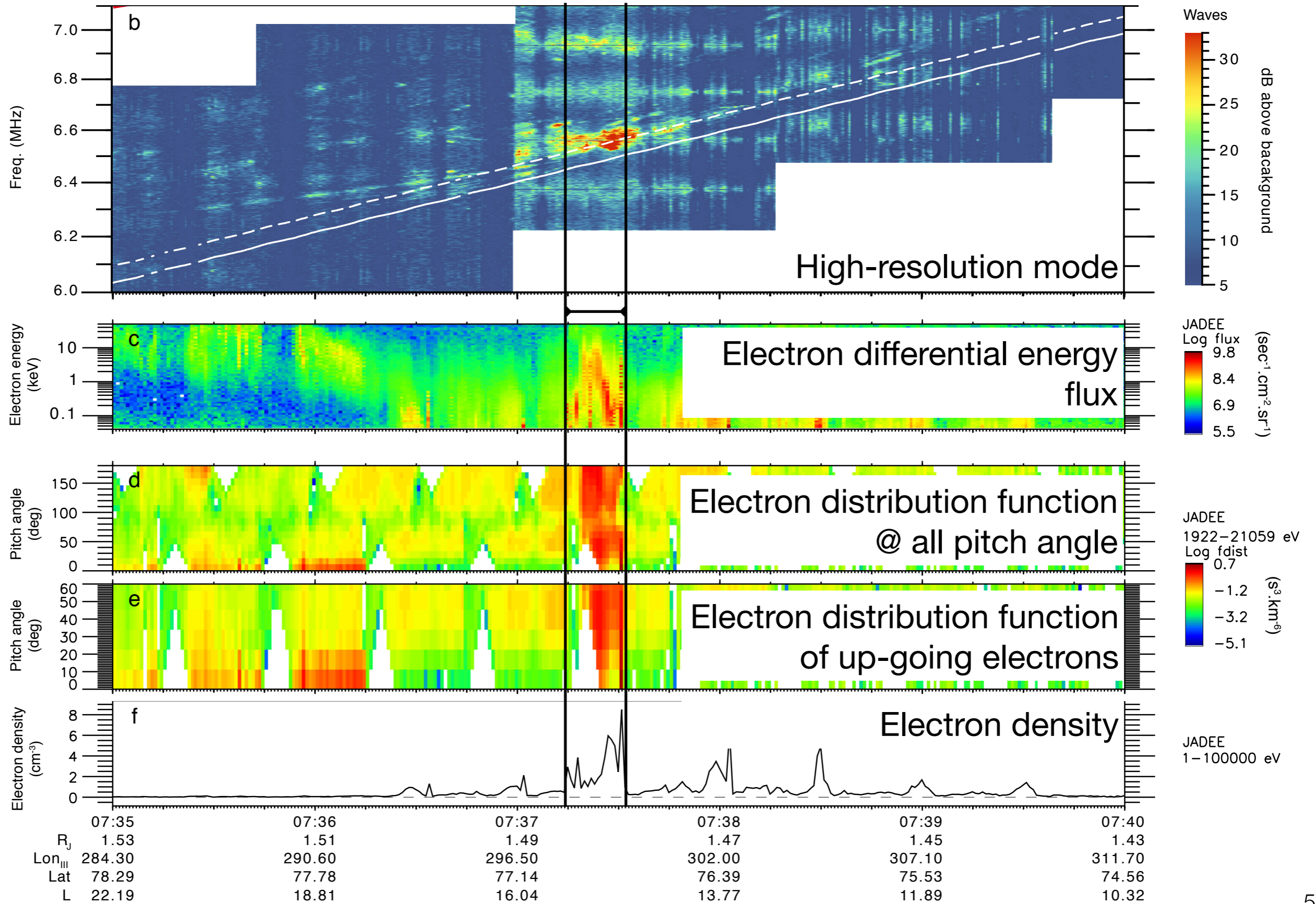
Figure 1. (top) UV false color of the auroral emissions near Juno's mapped magnetic footprint. Gray areas mark regions UVS either did not observe or registered no photons while viewing. Qualitatively, red features correspond to emissions deep in the atmosphere due to higher-energy precipitating electrons, while pink/white features correspond to higher-altitude emissions due to lower-energy incident electrons. (bottom) The color spectrogram shows JADE downward precipitating differential energy flux (DEF). The overlaid line shows energy flux (EF) within the loss cone, with the separate EF axis on the right of the spectrogram.

Juno/Waves data



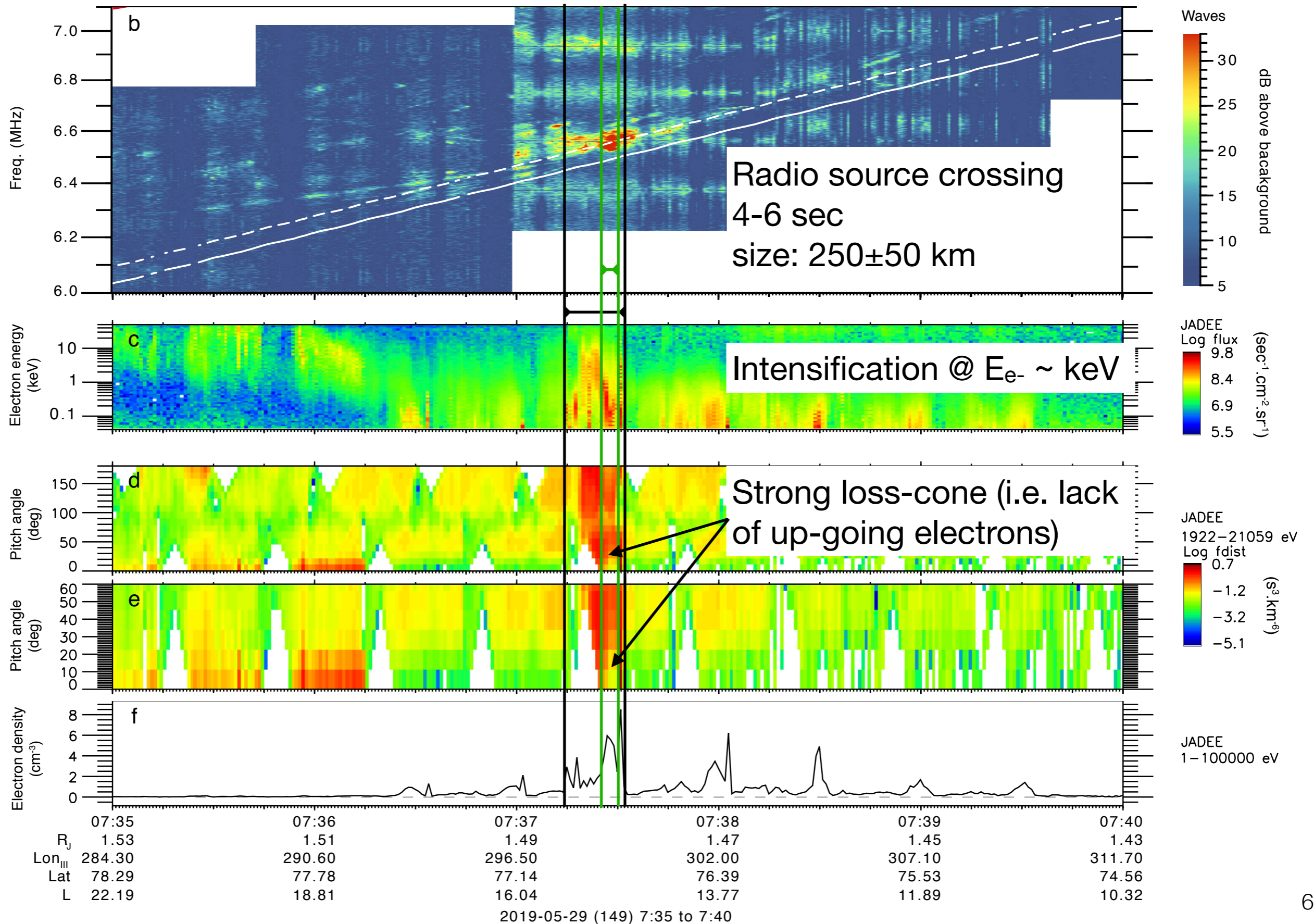
Juno/Waves & Juno/JADE-E data

[Louis et al., 2020]



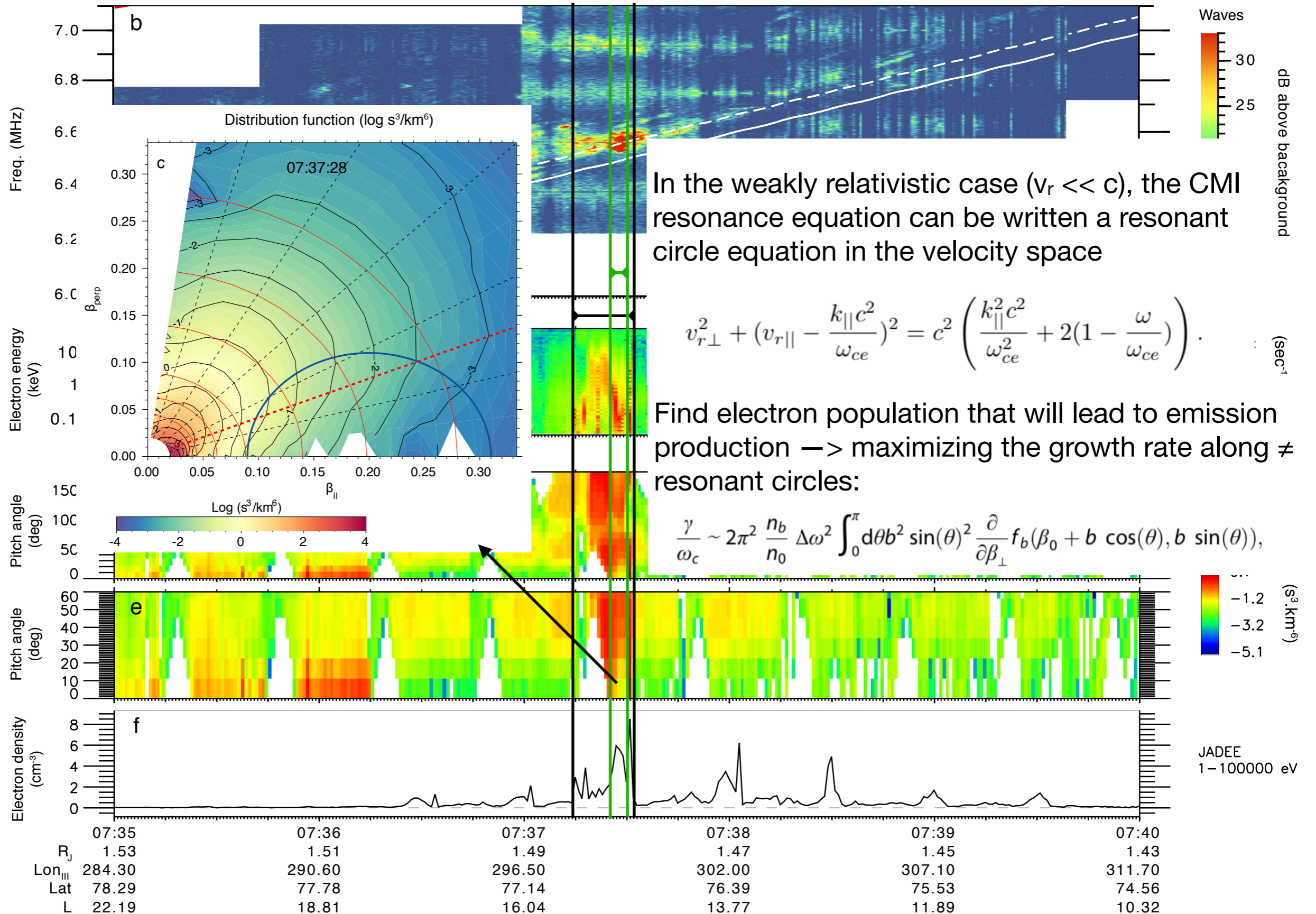
Juno/Waves & Juno/JADE-E data

[Louis et al., 2020]



Electron distribution function

[Louis et al., 2020]



In the weakly relativistic case ($v_r \ll c$), the CMI resonance equation can be written a resonant circle equation in the velocity space

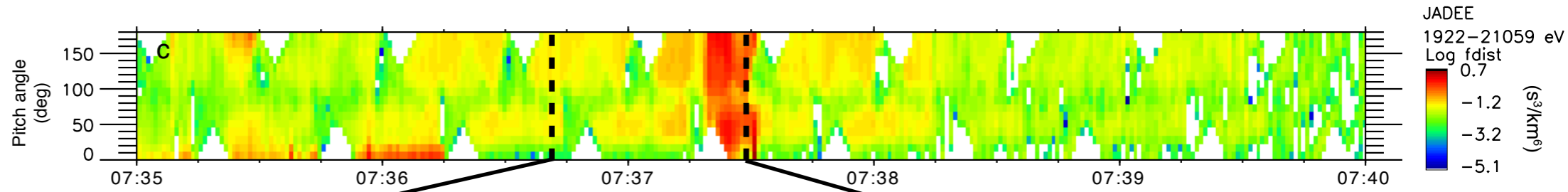
$$v_{r\perp}^2 + (v_{r\parallel} - \frac{k_{\parallel} c^2}{\omega_{ce}})^2 = c^2 \left(\frac{k_{\parallel}^2 c^2}{\omega_{ce}^2} + 2(1 - \frac{\omega}{\omega_{ce}}) \right) \quad (\text{sec}^{-1})$$

Find electron population that will lead to emission production → maximizing the growth rate along ≠ resonant circles:

$$\frac{\gamma}{\omega_c} \sim 2\pi^2 \frac{n_b}{n_0} \Delta\omega^2 \int_0^\pi d\theta b^2 \sin(\theta)^2 \frac{\partial}{\partial \beta_\perp} f_b(\beta_0 + b \cos(\theta), b \sin(\theta)),$$

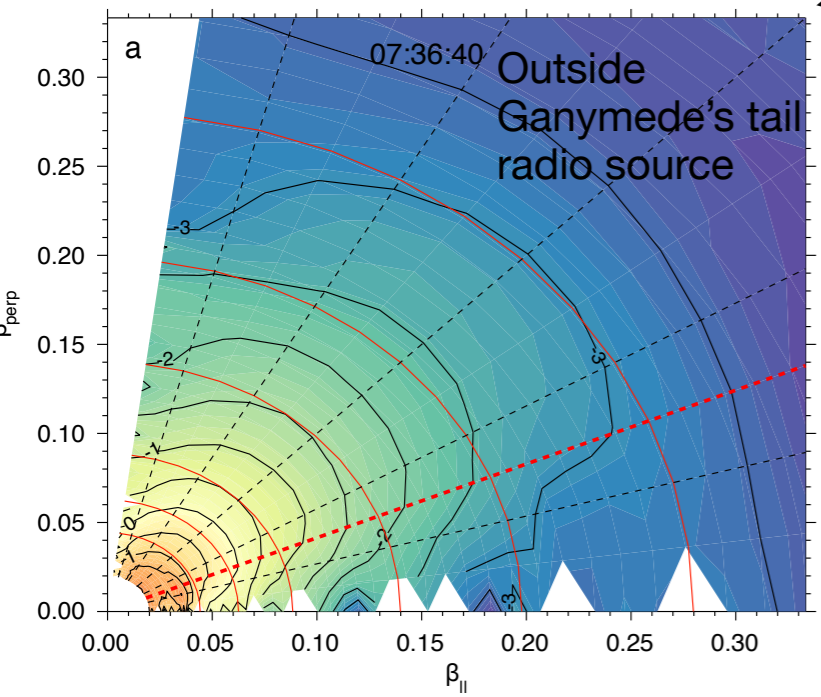
Emission characteristics

[Louis et al., 2020]



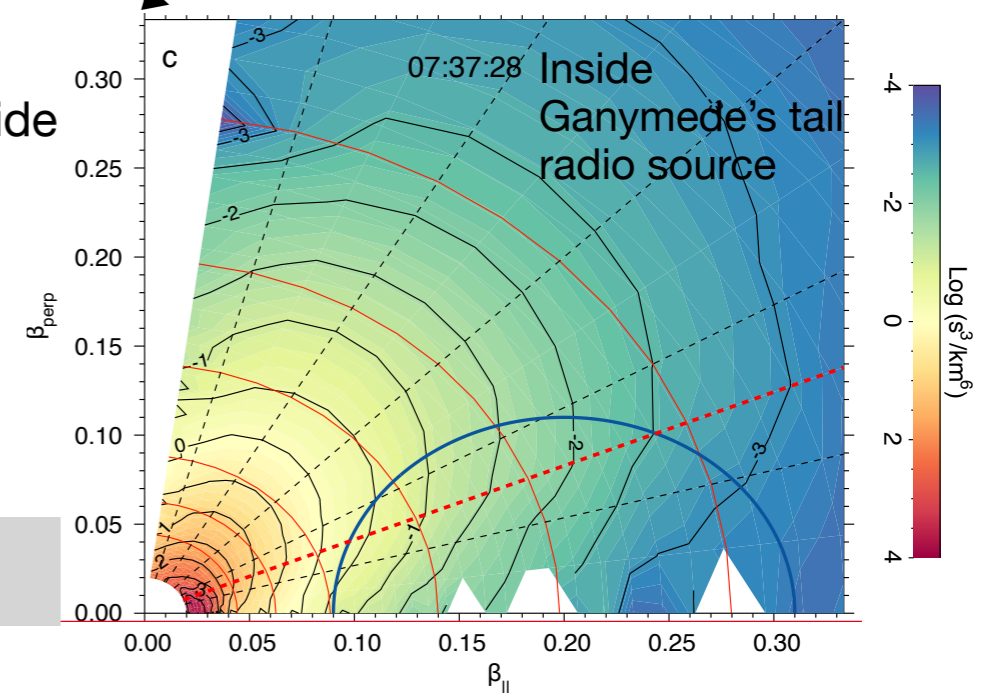
Distribution function (log s³/km⁶)

Distribution function (log s³/km⁶)



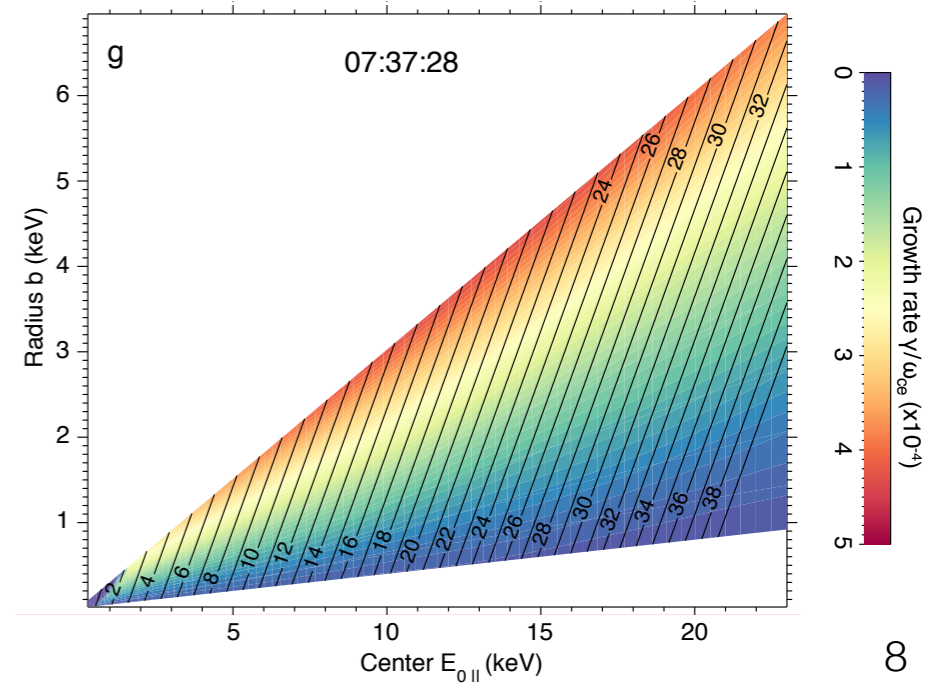
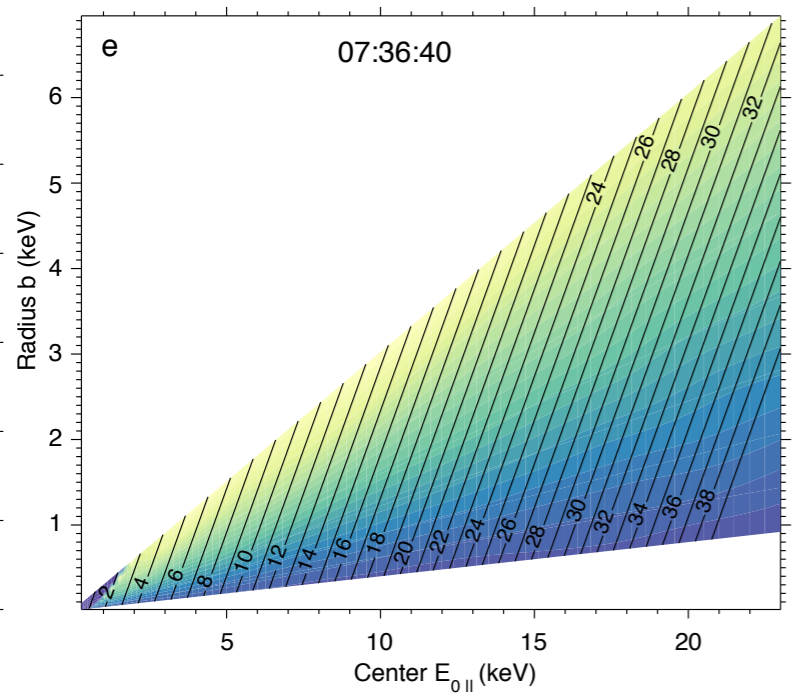
Electron distribution function: denser, hotter and more energized plasma inside radio source

In a source of ~100s km in size: growth rate of 3×10^{-4} sufficient to produce radio emission



Grow rate γ/ω_{ce} and $\Delta\omega$ iso-contour along resonant circles

Grow rate γ/ω_{ce} and $\Delta\omega$ iso-contour along resonant circles



	07:36:40	07:37:25 - 07:37:30
Loss Cone	Yes (~22.5°)	Yes (~22.5°)
Growth rate	$< 3 \times 10^{-4}$	$> 3 \times 10^{-4}$
Radio emission	No	Yes
Electron energy	∅	4-15 keV
f_{emission}	∅	$1.001 - 1.021 \times f_{ce}$
Opening angle	∅	76°-83°

Io's tail flux tube crossing

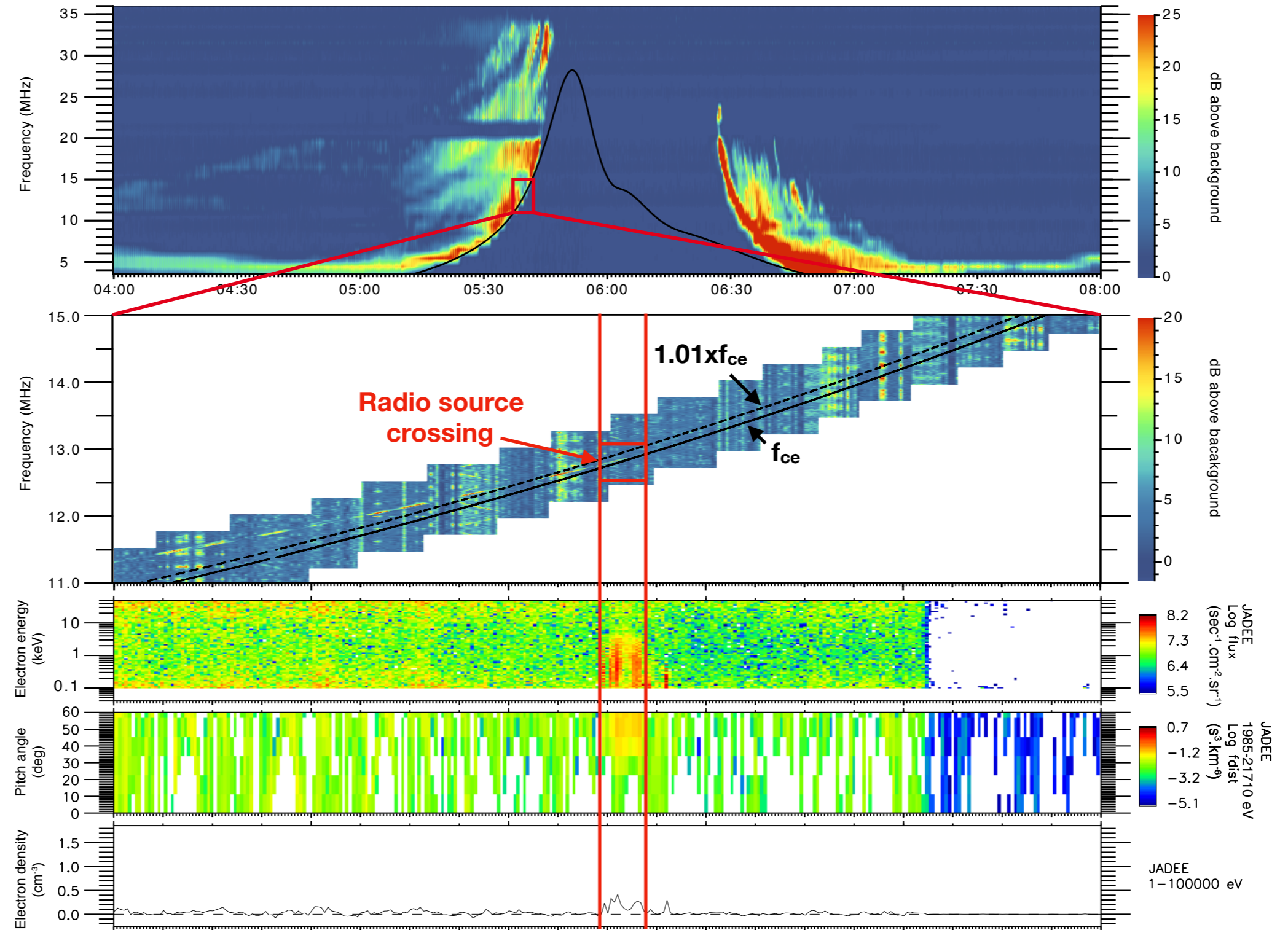
- 18 Io's tails flux tube crossing [Louis et al., 2019, Szalay et al., 2018, 2020b]
- FUV emission observed, sustained by Alfvénic acceleration processes

Day	Start (UTC)	Stop (UTC)	PJ	H	R (R _J)	Alt (R _J)	$\Delta\lambda_{\text{Lon}}$ (°)	$\Delta\lambda_{\text{Frac}}$ (°)	$\Delta\lambda_{\text{Alfvén}}$ (°)	Split	Width (D _{Io})	Radio emission observed	JADE upgoing e ⁻ data ?
2017-086	08:34:36	08:34:41	5	N	1.20	0.24	7	10	13		3.8	✓	✗
2017-086	09:30:51	09:31:02	5	S	1.65	0.70	6	3	4	✓	1.6	✓	✓
2017-139	05:39:28	05:39:48	6	N	1.27	0.31	40	65	91		5.7	✓	✓
2017-139	06:39:53	06:40:04	6	S	1.65	0.70	48	29	28	✓	1.5	✗	✓
2017-192	01:24:40	01:25:01	7	N	1.44	0.50	125	125	115		6.0	✗	✓
2017-192	02:22:27	02:22:54	7	S	1.40	0.44	70	88	90	✓	4.6	✗	✓
2018-091	09:20:37	09:20:54	12	N	1.34	0.39	2	6	2		4.0	✗	✓
2018-144	05:13:11	05:13:20	13	N	1.37	0.43	38	20	16		2.5	✗	✓
2018-197	04:49:50	04:50:12	14	N	1.39	0.45	96	80	57	✓	6.3	✗	✓
2018-250	00:48:14	00:48:27	15	N	1.30	0.36	151	68	67	✓	4.1	✗	✓
2018-250	01:46:00	01:46:17	15	S	1.54	0.58	51	67	62		3.2	✗	✓
2018-302	20:47:38	20:47:44	16	N	1.21	0.26	122	111	111		7.1	✗	✓
2018-302	21:46:45	21:47:20	16	S	1.69	0.74	100	135	114	✓	5.2	✗	✓
2019-255	03:18:52	03:19:07	22	N	1.31	0.37	4	3	5		6.1	✗	✓
2019-307	22:07:02	22:07:19	23	N	1.11	0.14	45	68	83		14.9	✗	✓
2019-307	23:10:38	23:10:56	23	S	1.96	1.01	35	31	31		1.9	✗	✓
2019-360	18:30:16	18:32:24	24	S	2.03	1.08	93	61	61		8.9	✗	✓
2020-101	14:34:57	14:37:36	26	S	1.88	0.93	170	127	134		12.8	✗	✓

Table S1. Close approach Io footprint tail crossings where JADE resolved the loss cone and detected appreciable fluxes. Start and stop times refer to the beginning/end of each feature; PJ – perijoves, H – hemisphere; R – radial distance; Alt. – altitude above ellipsoid; $\Delta\lambda_{\text{Lon}}$ – downtail angles; Split – split tail feature; width – equatorial width in Io diameters; SNR – signal to noise ratio for the addition of backgrounds; and EF_{peak} – peak energy flux.

Juno/Waves & Juno/JADE-E data

[Louis et al., in prep.]

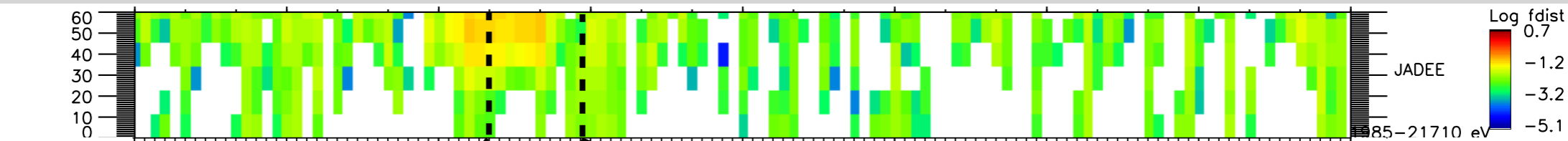


	05:37	05:38	05:39	05:40	05:41	05:42
R_J	1.31	1.30	1.28	1.26	1.24	1.22
Lon_{III}	122.70	123.50	124.30	125.10	125.80	126.60
Lat	62.40	60.70	58.94	57.14	55.28	53.36
$Mlat_{JRM09}$	63.48	62.05	60.56	59.00	57.37	55.69
MLT	18.09	17.99	17.89	17.80	17.71	17.63
L	6.60	5.90	5.28	4.74	4.27	3.85

2017-05-19 (139) 5:37 to 5:42

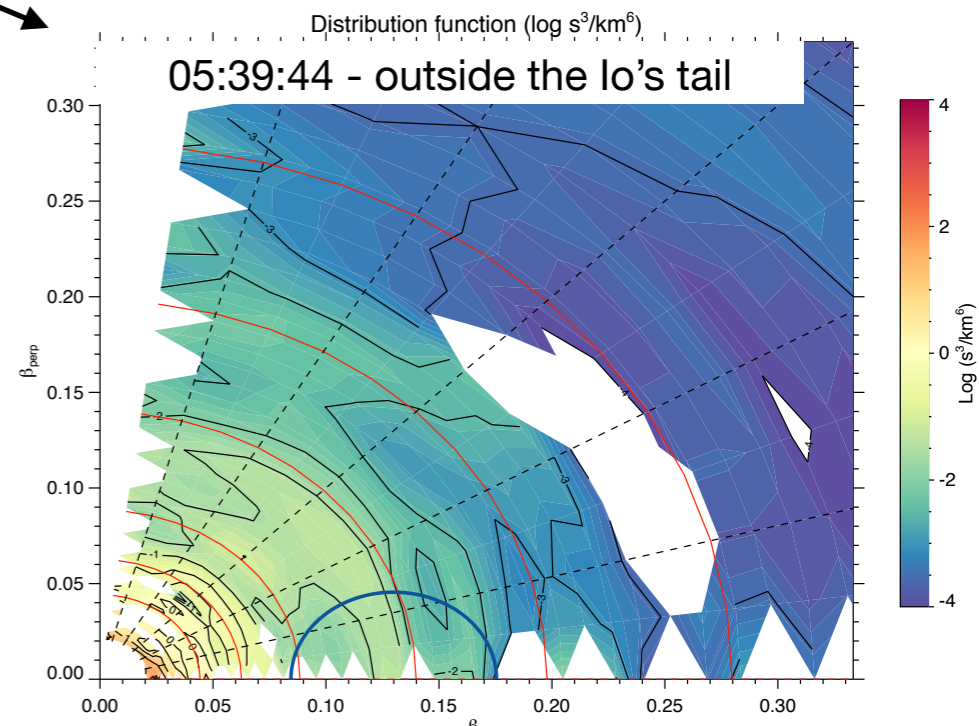
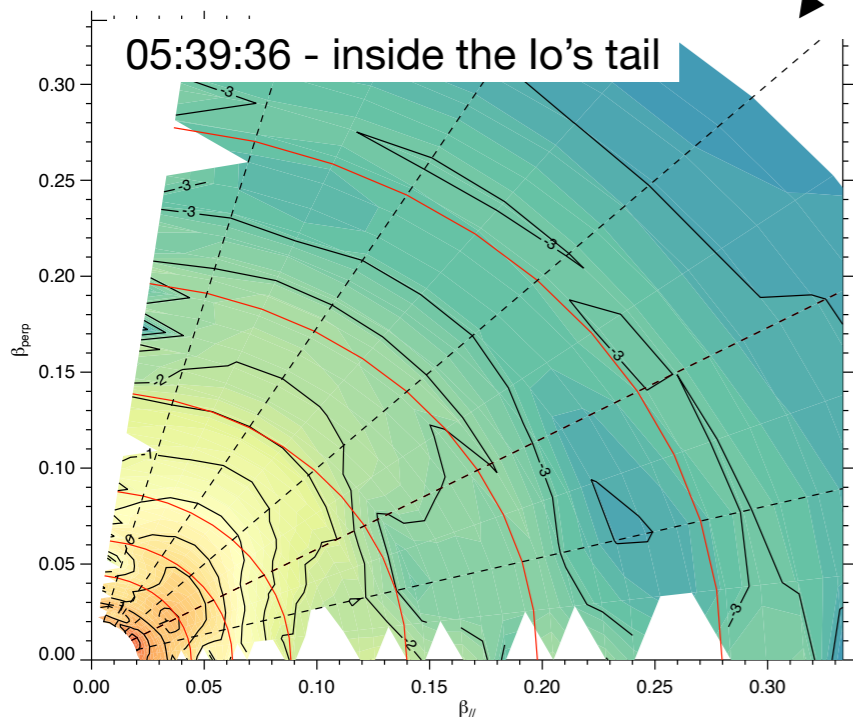
Juno/Waves & Juno/JADE-E data

[Louis et al., in prep.]

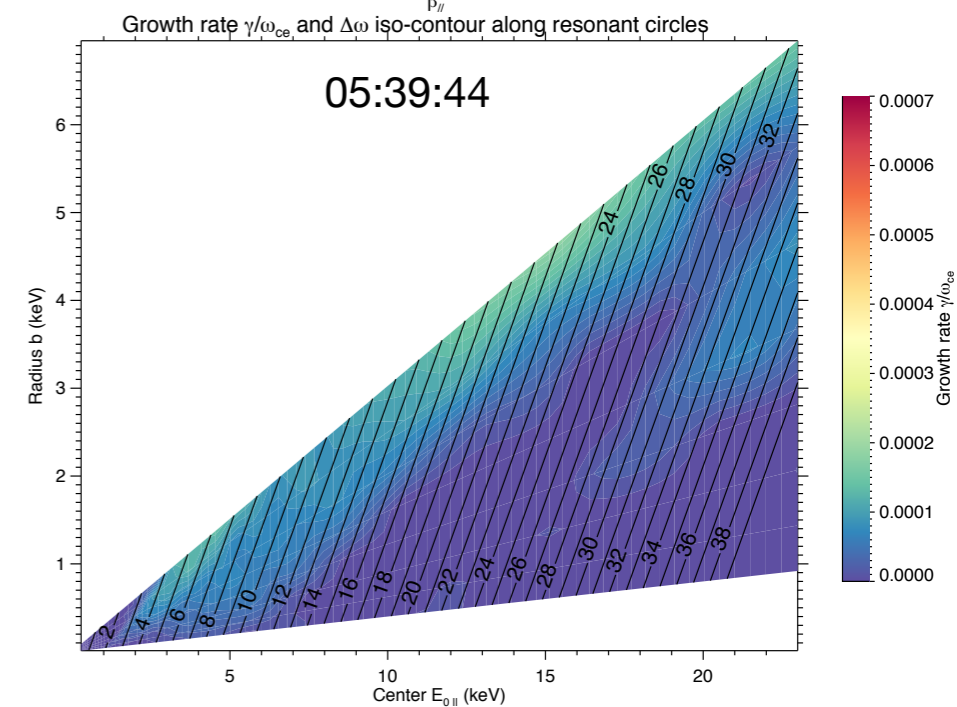
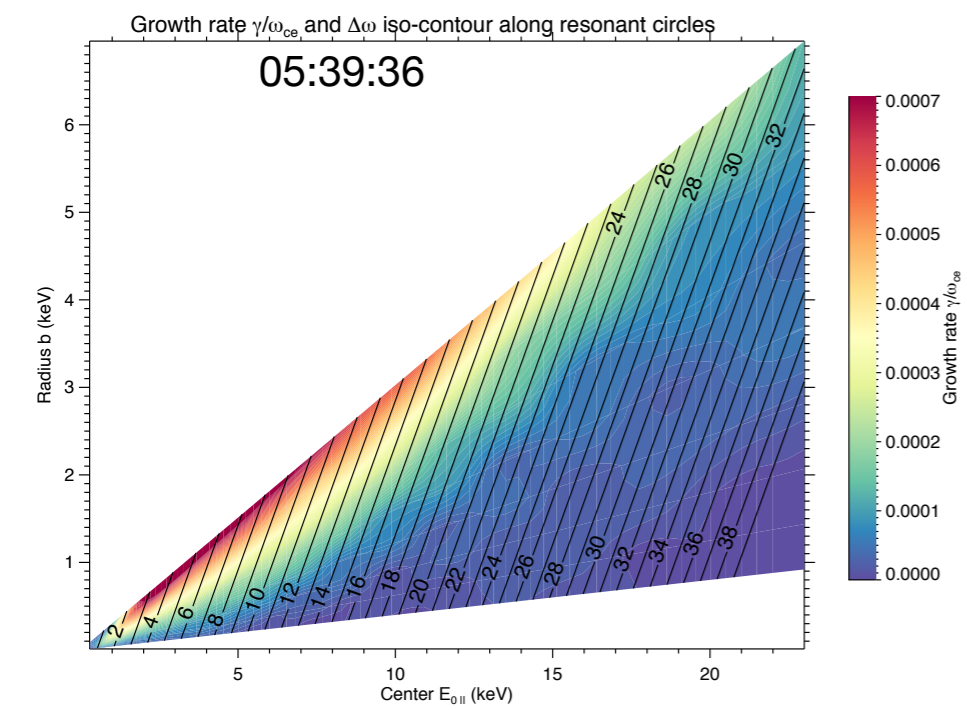


	05:39:00	05:39:15	05:39:30	05:39:45	05:40:00	05:40:15	05:40:30	05:40:45	05:41:00
R_J	1.28	1.28	1.26	1.26	1.26	1.26	1.24	1.24	1.24
Lon_{III}	124.30	124.30	125.10	125.10	125.10	125.10	125.80	125.80	125.80
Lat	58.94	58.94	57.14	57.14	57.14	57.14	55.28	55.28	55.28
$MLat_{JRM09}$	60.56	60.56	59.00	59.00	59.00	59.00	57.37	57.37	57.37
MLT	17.89	17.89	17.80	17.80	17.80	17.80	17.71	17.71	17.71
L	5.28	5.28	4.74	4.74	4.74	4.74	4.27	4.27	4.27

2017-05-19 (139) 5:39 to 5:41

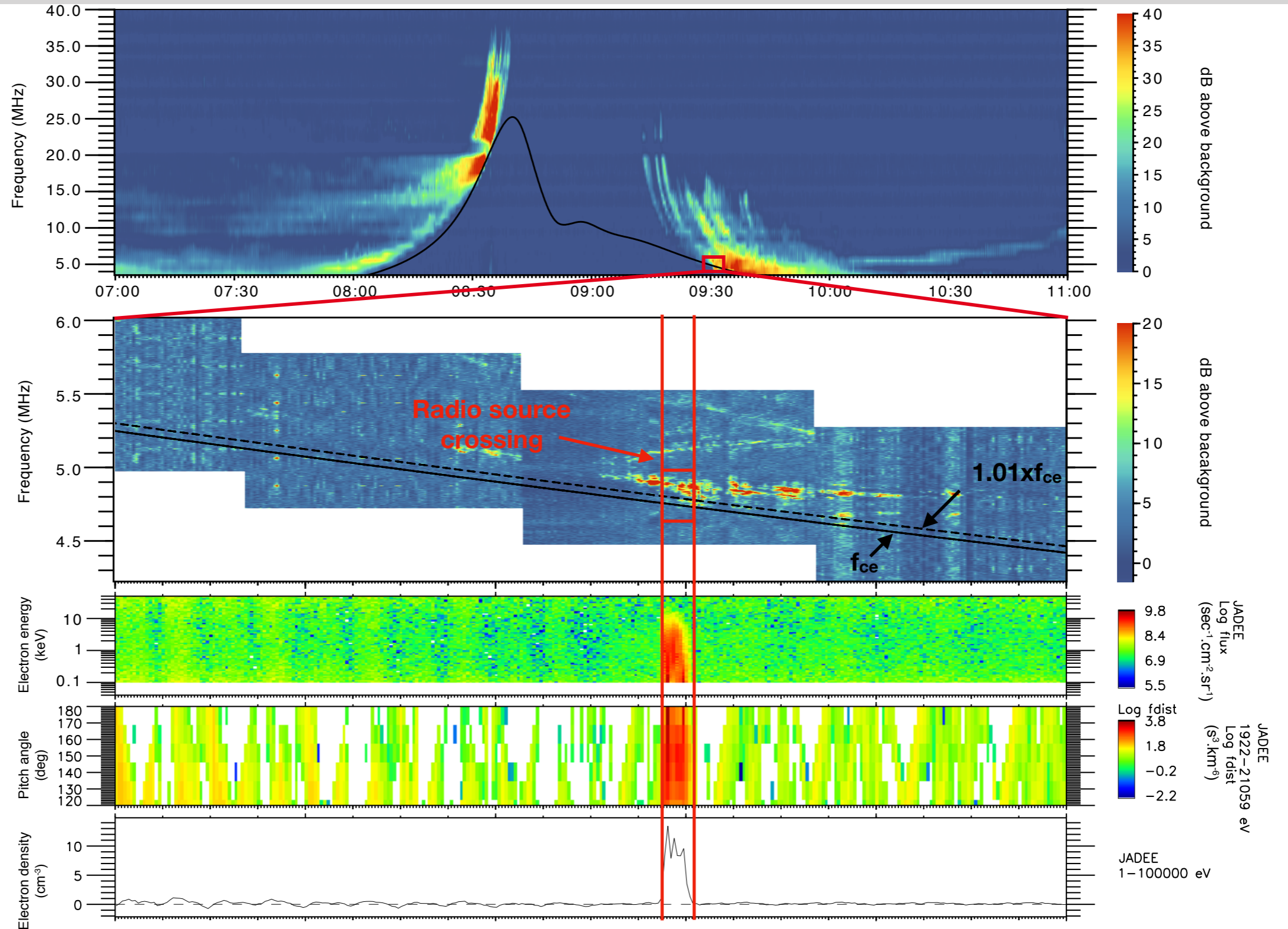


	05:39:31-05:39:39	05:39:45
Loss cone	Yes (~20-30°)	No
Growth rate	$>10^{-4}$	$<10^{-4}$
Radio emission	Yes	No
Electron energy	1-10 keV	\emptyset
$f_{emission}$	$(2-14 \times 10^{-3}\%) > f_{ce}$	\emptyset
Opening angle	77-86°	\emptyset



Juno/Waves & Juno/JADE-E data

[Louis et al., in prep.]

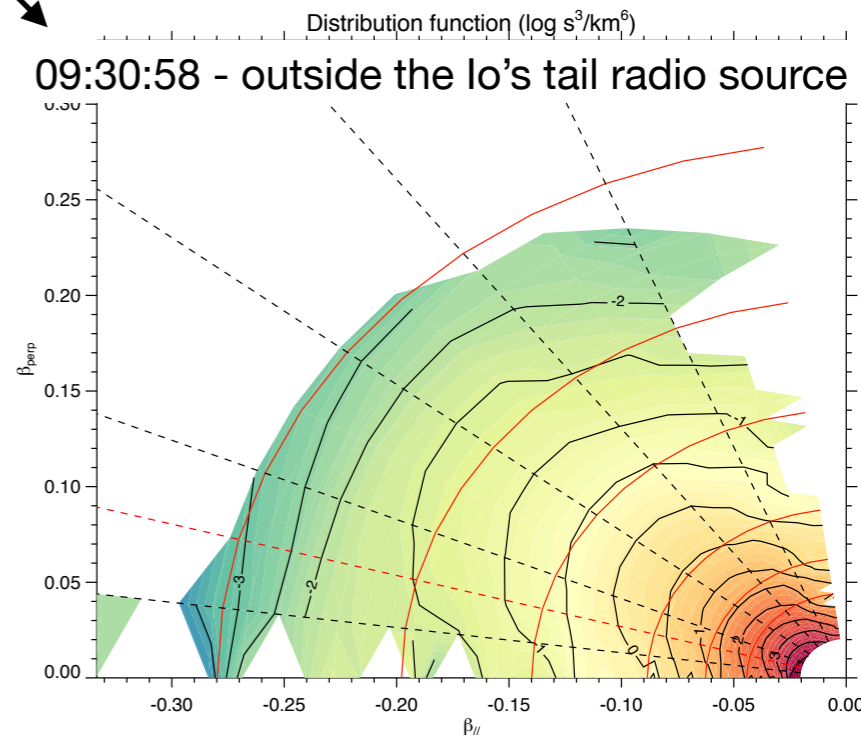
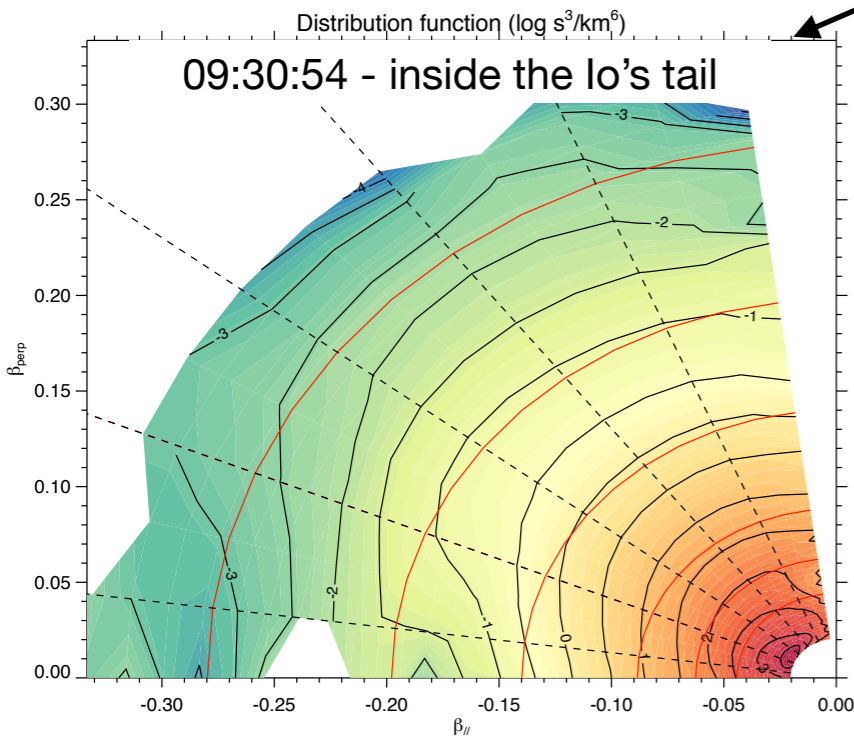
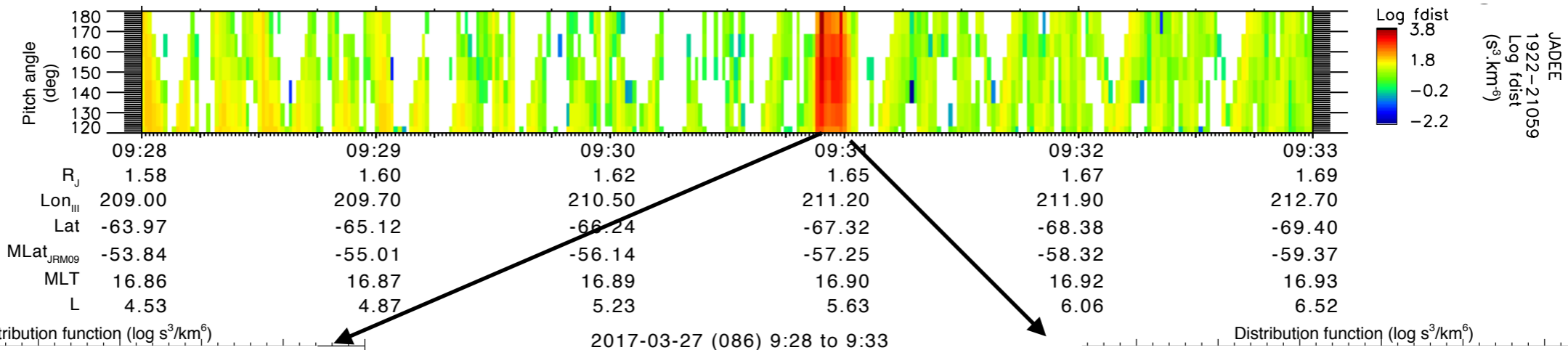


	09:28	09:29	09:30	09:31	09:32	09:33
R_j	1.58	1.60	1.62	1.65	1.67	1.69
Lon_{III}	209.00	209.70	210.50	211.20	211.90	212.70
Lat	-63.97	-65.12	-66.24	-67.32	-68.38	-69.40
$MLat_{JRM09}$	-53.84	-55.01	-56.14	-57.25	-58.32	-59.37
MLT	16.86	16.87	16.89	16.90	16.92	16.93
L	4.53	4.87	5.23	5.63	6.06	6.52

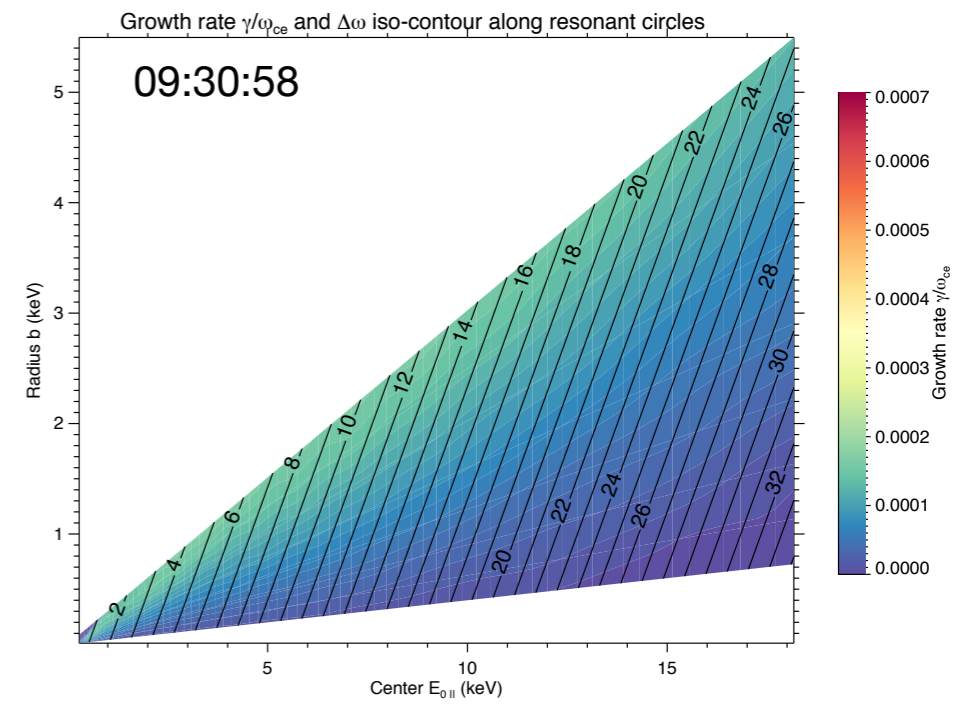
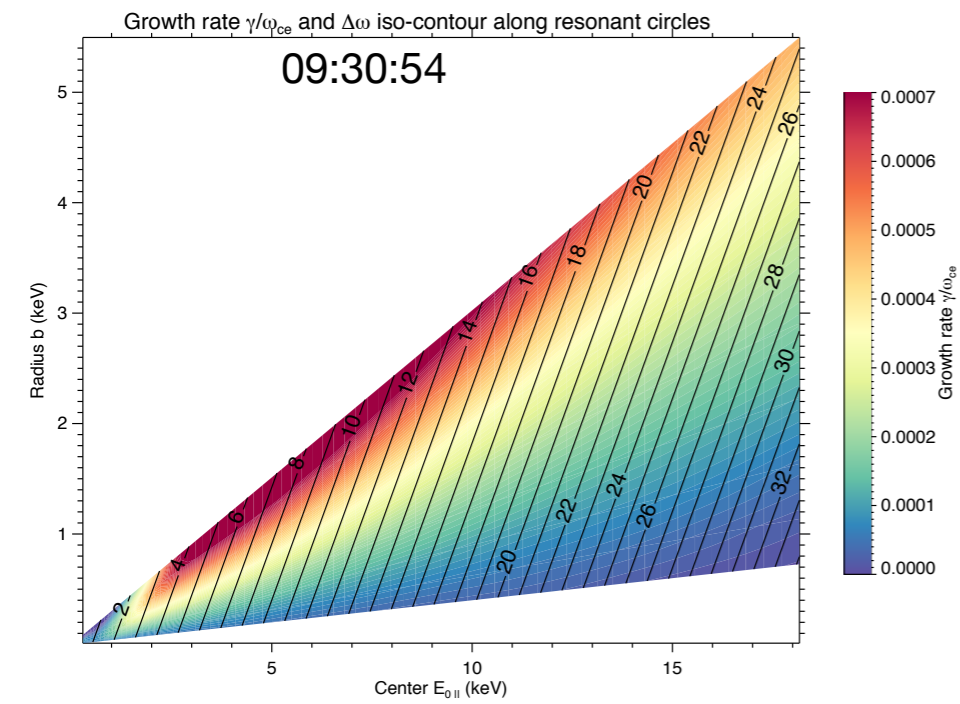
2017-03-27 (086) 9:28 to 9:33

Juno/Waves & Juno/JADE-E data

[Louis et al., in prep.]



	09:30:52-09:30:56	09:30:58
Loss cone	Yes (~30°)	Yes (~22.5°)
Growth rate	$>10^{-4}$	$<10^{-4}$
Radio emission	Yes	No
Electron energy	2-20 keV	\emptyset
$f_{emission}$	$(18-28 \times 10^{-3}\%) > f_{ce}$	\emptyset
Opening angle	74-85°	\emptyset



Europa's tail source crossing

- Europa's tail flux tube crossing [Allegrini et al., 2020]

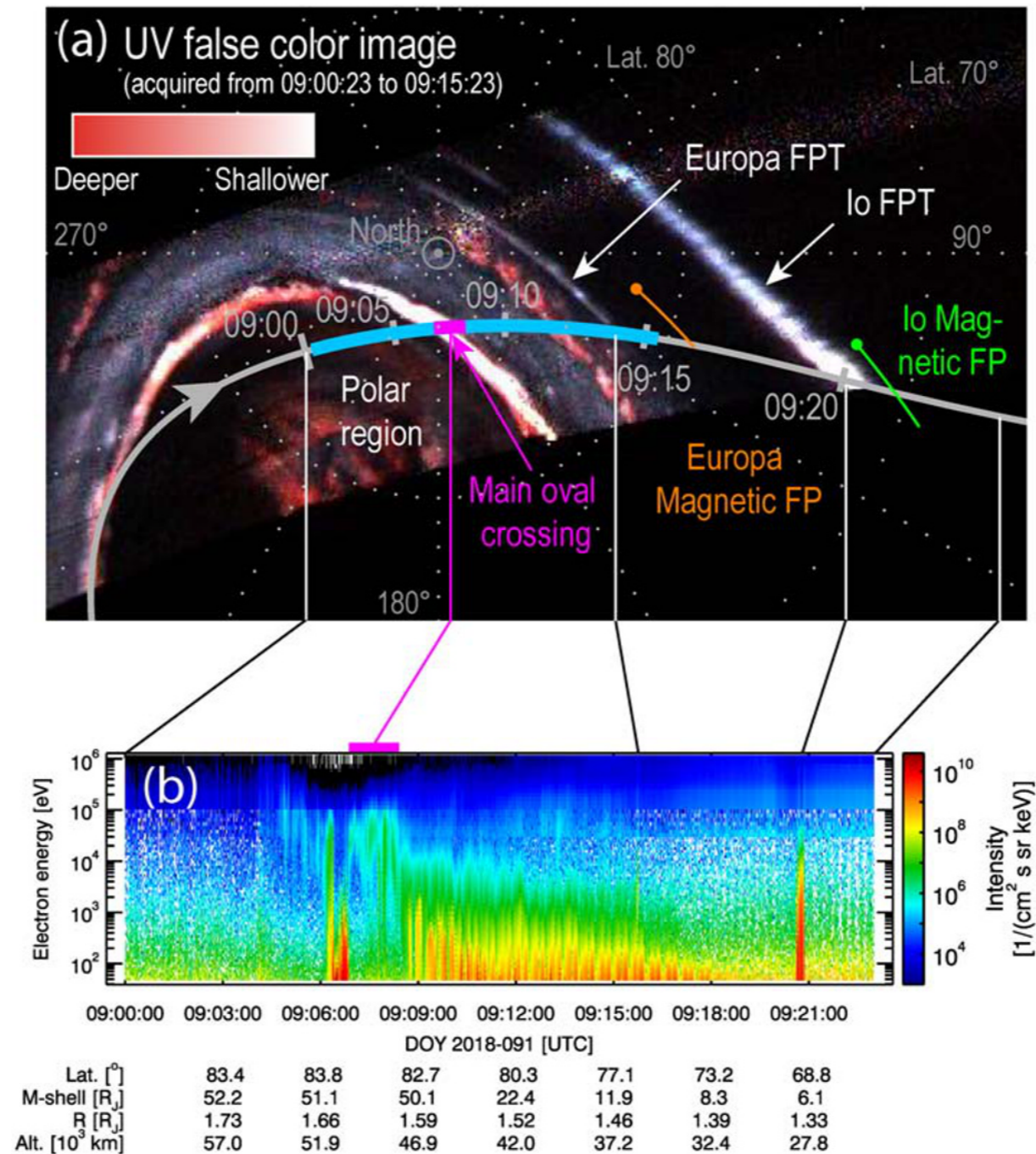
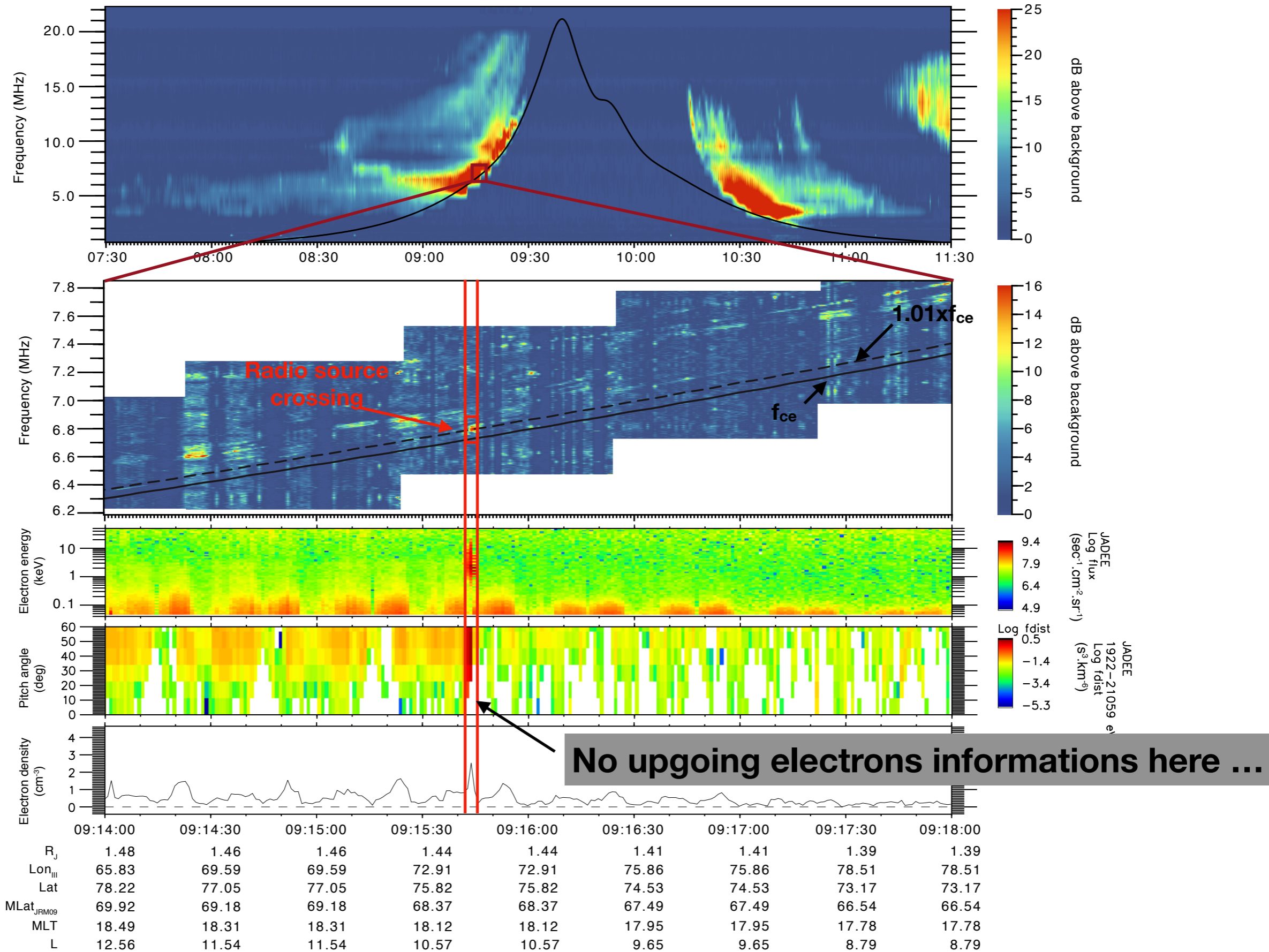
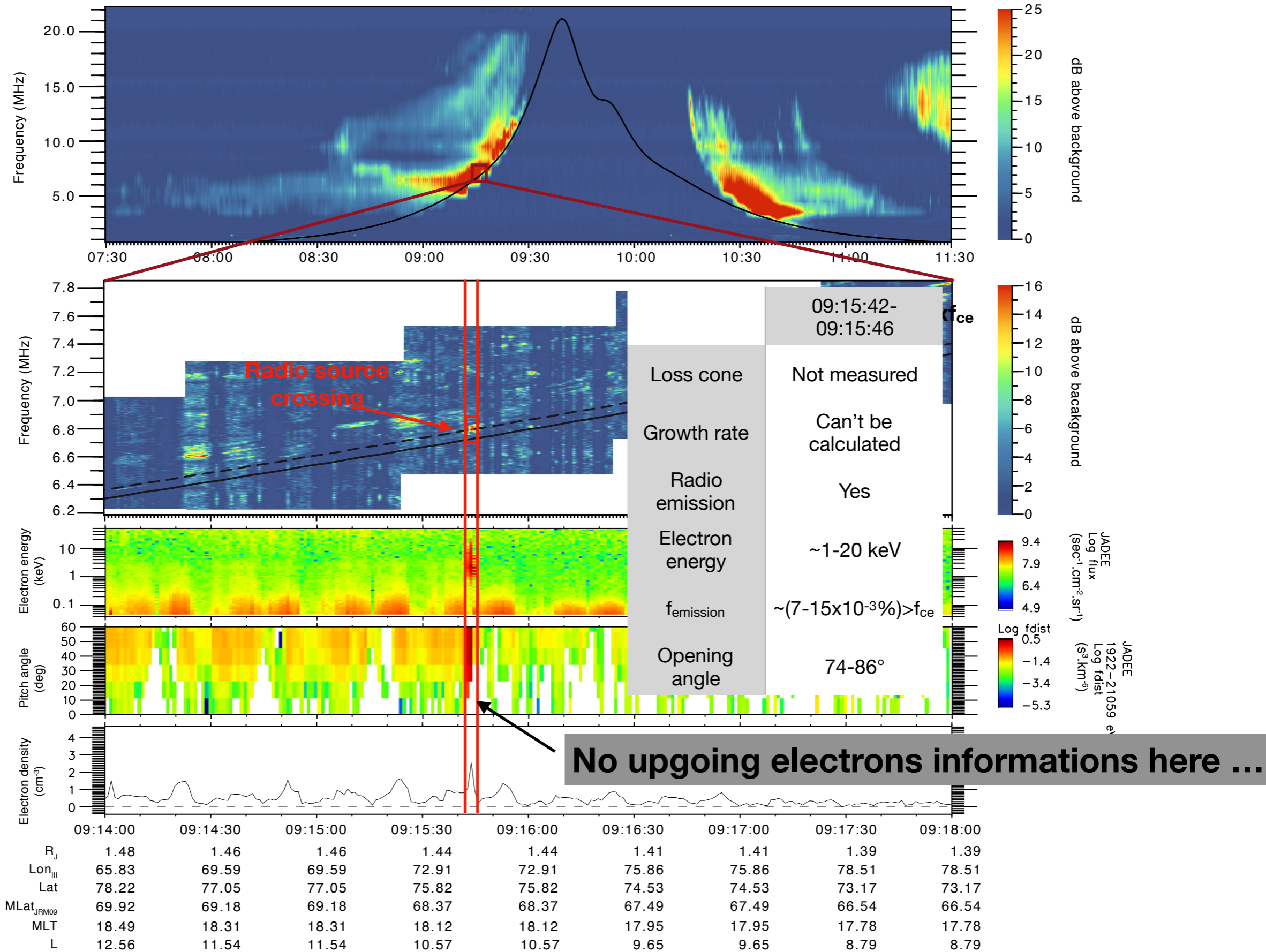


Figure 1. (a) UVS reconstructed false color image acquired from 09:00:23 to 09:15:23. The color is related to the depth of the emission where red comes from deeper in the atmosphere. Juno's magnetic footprint track is shown in gray and in light blue during the image acquisition. Europa and Io's magnetic footprints are shown in orange and green, respectively, using JRM09 + CAN1981. (b) Combined JADE and JEDI electron energy spectrogram from 50 eV to 1 MeV. The spacecraft jovigraphic latitude, M-shell, radial distance, and altitude above the 1-bar level are indicated below panel (a). The lines between the panels connect the features from the image (not the magnetic footprints) in panel (a) to their corresponding electron measurements in panel (b). There are discrepancies between the crossing times of the mapped UV features and the corresponding signatures in the electron data. For example, the Europa tail crossing in panel (a) occurs before 09:15 but is measured in the electrons after 09:15. More details are found in the text.

Juno/Waves & Juno/JADE-E data



Juno/Waves & Juno/JADE-E data



Conclusion & Perspectives

→ Ganymede

- Ganymede-induced radio emission triggered by loss-cone-driven-CMI
- Radio source size: 250 km
- Resonant Electron energy: 4-15 keV
- Beaming angle $\theta = [76^\circ-83^\circ]$
- Radio emission associated with a Ganymede down-tail FUV emission (likely one of the Reflected Alfvén Wing spot, as for Io)

→ Io:

- Io-induced radio emission triggered by loss-cone-driven-CMI
- Radio source size: $\sim 415 \pm 50$ km / $\sim 185 \pm 46$ km
- Resonant Electron energy: 1-10 keV / [2-20] keV
- Beaming angle $\theta = [77^\circ-86^\circ] - [74^\circ-85^\circ]$
- Radio emission associated with a Io down-tail FUV emission (likely one of the Reflected Alfvén Wing spot, one very close to the MAW, the other at $\Delta\lambda_{\text{Alfvén}} \sim 90^\circ$)

→ Europa:

- Radio source size: $\sim 200 \pm 49$ km ?
- Resonant Electron energy: 1-20 keV (?)
- Beaming angle $\theta = [74^\circ-86^\circ]$ (?)
- Radio emission associated with a Europa down-tail FUV emission (likely one of the Reflected Alfvén Wing spot)

Conclusion & Perspectives

- ➔ Cyclotron Maser Instability:
 - Loss-cone-driven CMI: common way to amplify waves and produce radio emission, sustained by an Alfvénic acceleration process:
 - in the case of auroral radio emissions [*Louarn et al., 2017; 2018*]
 - in the case of moon-induced radio emission [Louis et al., 2020 and this presentation]
 - CMI needs dense, hot, energetic plasma to occurs (no radio emission crossed during the beginning of the Ganymede's tail flux tube crossing when n_e is lower)

- ➔ Next steps:
 - Why radio emission is not observing each time we crossed the Io flux tube?
 - How radio emission can be produced 10s of degree away from the MAW?
 - How the electron distribution function and the radio emission intensity evolved with distance from the MAW?
 - Wait for more moon flux tube crossing, during which we could observe radio emission..

Thank you for your attention

